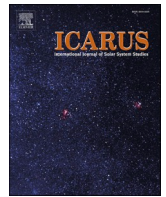




Contents lists available at ScienceDirect

Icarus

journal homepage: www.elsevier.com/locate/icarus

Recent faulting at the Claritas Rupes scarp on Mars

Bartosz Pieterek^{a,b,*}, Petr Brož^c, Ernst Hauber^d

^a Polish National Institute – National Science Institute, Warsaw, Poland

^b Geohazard Lab, Institute of Geology, Adam Mickiewicz University, Poznań, Poland

^c Institute of Geophysics of the Czech Academy of Sciences, Prague, Czech Republic

^d Institute of Planetary Research, DLR, Berlin, Germany

ARTICLE INFO

Keywords:

Thaumasia
Volcanism
Subsidence
Boulders
Neotectonics

ABSTRACT

Endogenic processes have greatly affected the Martian surface, especially concentrating at several volcano-tectonic centers. The formation of Tharsis, a vast volcanic bulge, significantly influenced the western hemisphere of Mars. The associated loading stresses caused the formation of various sets of tectonic structures that might have remained active until today. However, surface evidence for very recent endogenic processes in Tharsis is sparse. Here, using the Context Camera (CTX) and High Resolution Imaging Science Experiment (HiRISE) images, we report the presence of fresh-appearing systems of local-scale scarps mostly developed at the southern edge of Tharsis, specifically at Claritas Rupes scarp. These scarps are spatially associated with depression centers situated at the base of Claritas Rupes, inside the Thaumasia Graben which is partially filled by volcanic deposits. The relationships between the studied scarps and present-day surficial processes and its deposits such as rockfalls indicate a young age of the scarps' development, namely, in the range of <1 Ma. The pristine topography (sharp and thin ridges), spatial distribution (association with depression centers), and regional geological context of Claritas Fossae lead us to interpret these scarps as surficial expressions of tectonic activity attributed to normal faulting. This could be related to Deep-seated Gravitational Slope Deformations (DGSDs) released by seismic activity related to ongoing subsidence of depression centers and/or reactivation of the listric normal Claritas Rupes fault. These observations imply that this region experienced long-lasting and multiple volcano-tectonic events and the formation of the youngest deformations could represent neotectonic activity, which has been active until recently, and possibly might be still ongoing.

1. Introduction

The investigation of structural features on the surface of Mars has shown that the tectonic activity has progressively reduced through time (Carr and Head III, 2010; Golombek and Phillips, 2010). Nevertheless, the present-day seismic evidence detected by NASA's InSight mission suggests that Mars is still seismically and/or tectonically active (e.g., Giardini et al., 2020; Stähler et al., 2022; Lognonné et al., 2023). One center of current endogenic activity seems to be spatially associated with the Cerberus Fossae region (Ceylan et al., 2023), which may be located above a magmatically active zone (e.g., a dike; Rivas-Dorado et al., 2022). However, the location of other seismically active centers is still poorly constrained due to low Marsquakes magnitudes, large epicentral distances, and background noise (Stähler et al., 2024). Therefore, the identification of very recent (<1 Ma) tectonic surface deformation as evidence of current endogenic activity would provide critical constraints

on the plausible location of Marsquakes and the tectonic evolution of the planet.

The formation of Tharsis, the largest volcanic province that covers a significant part of the western hemisphere of Mars (Fig. 1a), had a profound effect on Martian geodynamics (Bouley et al., 2018; Mougins-Mark et al., 2021). Although Tharsis-induced loading stresses that have accumulated within the Martian crust caused widespread fracturing and crustal deformations in the past (Cailleau et al., 2003; Andrews-Hanna et al., 2008; Bouley et al., 2018), there is a lack of evidence for recent tectonic activity associated with this volcanic province. As inferred through the age determinations of lava flows, endogenic activity at Tharsis persisted at least until the Late Amazonian (<300 Ma; Hauber et al., 2011; Richardson et al., 2021; Pieterek et al., 2022). The Late Amazonian-age magmatism (even <50 Ma) suggests that volcano-tectonic activity might have continued at Tharsis until recently, and that surface evidence of such activity might be still visible and

* Corresponding author at: Polish National Institute – National Science Institute, Warsaw, Poland.

E-mail address: bpieterek94@gmail.com (B. Pieterek).

<https://doi.org/10.1016/j.icarus.2024.116198>

Received 29 January 2024; Received in revised form 21 June 2024; Accepted 21 June 2024

Available online 25 June 2024

0019-1035/© 2024 The Authors. Published by Elsevier Inc. This is an open access article under the CC BY-NC-ND license (<http://creativecommons.org/licenses/by-nc-nd/4.0/>).

detectable with the use of satellite image datasets (Krishnan and Kumar, 2022). Yet, there is a general lack of evidence supporting this notion. To date, only very few morphologically pristine tectonic structures in Tharsis have been documented on a qualitative basis (i.e. inferred from sharp breaks in slope, distinct and sharp crests of scarp shoulders, and no or very little evidence of erosion) and inferred as evidence of young tectonic activity (Karimova et al., 2017; Kumar et al., 2019). The determination of absolute (model) ages of small-scale linear tectonic features is also difficult and even often impossible due to the limitations of the crater counting methods (e.g., Warner et al., 2015). The chronology of the recent tectonic evolution of Tharsis is therefore poorly constrained. Consequently, in the subsequent text, we use relative terms such as “young/recent” and “old/ancient” for features whose formation age is not clearly determined. This is because their small sizes limit the usage of absolute dating techniques in the form of crater counting, so only relative dating is available. However, when the terms “young/recent” and “old/ancient” are used in the text, they refer to a period of <1 Myr and >1 Gyr, respectively.

The fresh-appearing scarps have been recently detected in the northwest of Alba Mons (Karimova et al., 2017) and within Valles

Marineris (Kumar et al., 2019). These surface observations may indirectly support the detection of seismic events around Tharsis (Horleston et al., 2022; Zenhäusern et al., 2022; Ceylan et al., 2023) (Fig. 1a). However, the majority of distant seismic detections of tectonic events in Tharsis may be obscured from the InSight records due to the large size of the Martian core and its shadow (Stähler et al., 2021). Moreover, our direct insight into the volcano-tectonic evolution of Mars is strongly limited by the short time span of the available seismic data delivered by the InSight seismometer. Therefore, current evidence of recent (<1 Ma) volcano-tectonic activity and the dynamics of endogenic processes in Tharsis are fundamentally unknown and may only come from remotely sensed data.

In this study, we follow up on our previous work (Pieterik et al., 2024) on volcano-tectonic landforms in the Claritas Fossae region in the southeastern part of Tharsis (Fig. 1). This region has a complex history of faulting (Dohm and Tanaka, 1999; Dohm et al., 2001) and was subjected to multiple subsequent volcano-tectonic events that have contributed to its present-day geological settings (Balbi and Marini, 2024; Balbi et al., 2024; Pieterik et al., 2024). In addition to surface observations, thermal modelling of the Martian mantle conducted by Plesa et al. (2018, 2023)

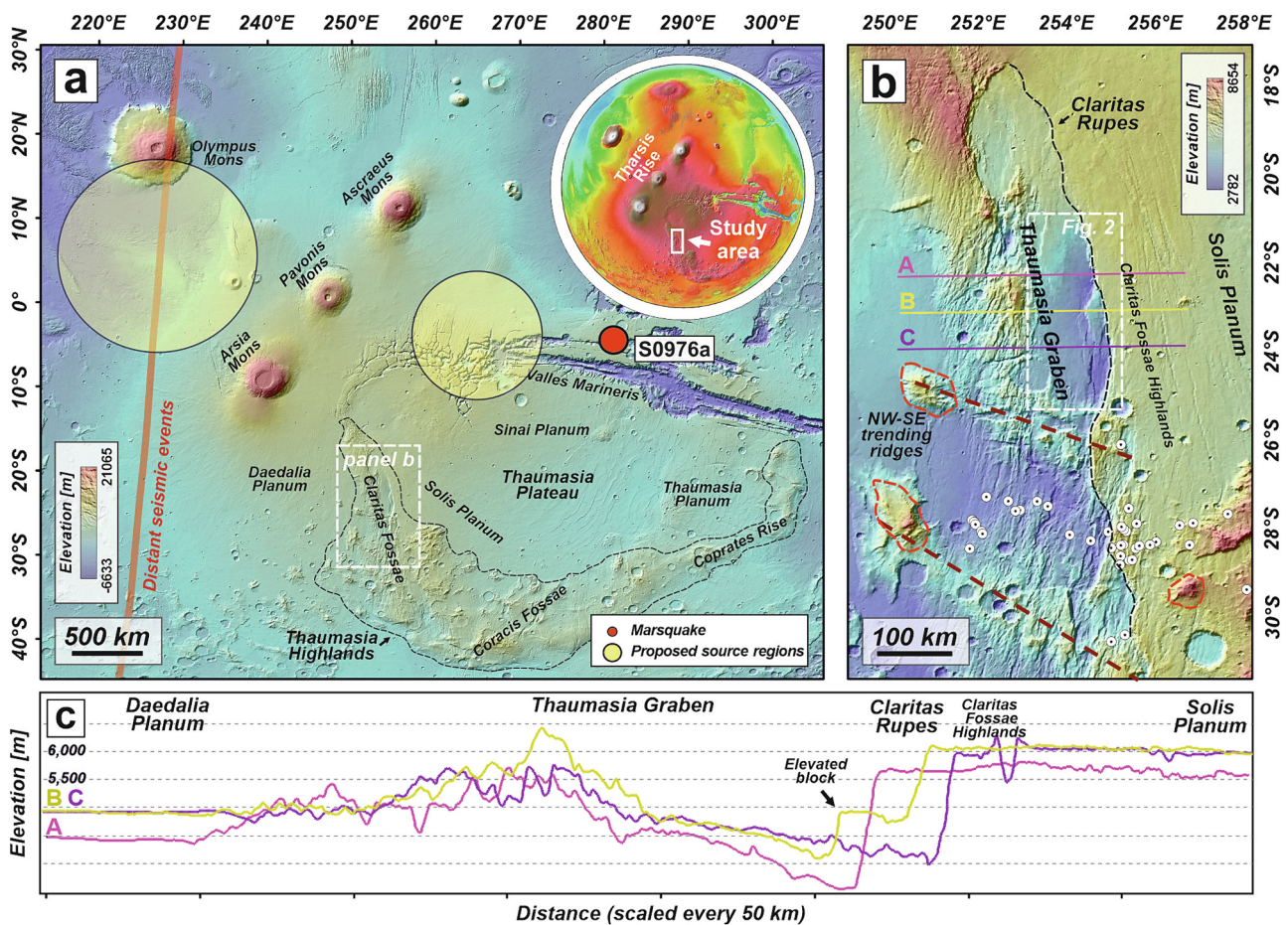


Fig. 1. (a) The middle top inset shows the location of Tharsis Rise and the study area to the southeast (white rectangle) on the topographic map of Mars. Schematic map of the Tharsis Volcanic Province including Thaumasia region and Claritas Fossae, which constitute the region of interest in this study. Marked by yellow-shaded circles are positions of proposed source regions of seismic activity of the distant events interpreted for Tharsis (Ceylan et al., 2023). Symbol sizes indicate the extent of the region, not location uncertainties. The red dot marks the position of one particular Marsquake and thick, orange line highlights the boundary of the area for which seismic activity is interpreted as distant events. The black dashed line marks the extent of Thaumasia Highlands. (b) Close up view of Claritas Fossae region, which hosts the large Thaumasia Graben and the NW-SE-trending ridges (brown, thick dashed lines) perpendicularly oriented to the main faults and tectonic structures of the region. The red dashed line marks the location of the hypothesized large-scale volcanoes (Dohm and Tanaka, 1999), whereas the white dots indicate the locations of small-scale volcanic edifices (Pieterik et al., 2024). The multicolour lines highlight the trace of the profile lines along which the topographic profiles in panel (c) were produced. The background map is a blend of the MOLA-HRSC digital elevation model and a global daytime infrared mosaic of THEMIS. (c) The corresponding topographic profiles (18 × vertically exaggerated) of the Claritas Fossae region that show the offset of the Claritas Rupes scarp and highlight the architecture of the large Thaumasia Graben. Produced using the MOLA MEX – HRSC global blended digital elevation model. (For interpretation of the references to colour in this figure legend, the reader is referred to the web version of this article.)

shows that assuming a pronounced crustal thickness dichotomy with homogenous crustal density, the highest present-day melt fractions on Mars may occur directly beneath the Claritas Fossae and Syria Planum regions. Hence, Claritas Fossae constitutes a promising target for searching for evidence of recent volcano-tectonic activity in Tharsis.

As part of our mapping campaign related to the fresh-appearing volcanic edifices in Claritas Fossae (Pieterik et al., 2024), we specifically searched for pristine structural landforms. Here, we report on uphill-facing scarps developed on prominent, west-facing scarp (Claritas Rupes) that bounds a major extensional structure (informally termed Thaumasia Graben; Hauber and Kronberg, 2005) (Fig. 1b). Using the available images of the highest resolution acquired by the High Resolution Imaging Science Experiment (HiRISE), these newly identified scarps show a clear spatial relationship with recent rockfalls, allowing us to constrain their relative formation age. In addition to this, we investigate pristine scarps on the floor of the Thaumasia Graben which show a spatial relation with possible magmatic features and local zones of topographic subsidence. Unfortunately, we were not able to identify any morphological changes between HiRISE images acquired at different times, so if there is a very recent tectonic surface activity in this region, it must be older than at least 20 years and hence is unrelated to any InSight seismic event detections. Thus, our satellite image-based morphological investigations focusing on fresh-looking structural landforms show great advances in tectonic feature mapping, providing insight into inaccessible by direct measurements of subsurface endogenic processes in southeastern Tharsis.

2. Geological setting

The study area (centered at $\sim 23^\circ\text{S}$ and $\sim 255^\circ\text{E}$) is situated in the northwestern part of the Noachian-Hesperian Thaumasia highland belt (Anderson et al., 2001), which surrounds the Thaumasia plateau on the south and west (Fig. 1). This belt of highlands consists of three segments: Claritas Fossae (formed from 4.2 to 3.4 Ga; Vaz et al., 2014), Coracis Fossae (from 3.9 to 3.5 Ga; Grott et al., 2005), and Coprates Rise (from 4.1 to 3.0 Ga; Schultz and Tanaka, 1994; Dohm and Tanaka, 1999). The Claritas Fossae region constitutes a densely cratered and fractured highland belt segment that has been formed by several episodes of tectonic events (Hauber and Kronberg, 2005; Balbi and Marini, 2024; Balbi et al., 2024). These episodes resulted in the formation of a complex system of faults, grabens, and halfgrabens (Vaz et al., 2014). The most intensive tectonic activity in Claritas Fossae occurred in the Noachian (Anderson et al., 2001; Dohm et al., 2001) and progressively decreased during the Late Noachian and Early Hesperian before it further substantially lessened during Late Hesperian/Early Amazonian (Balbi et al., 2024). The absolute model ages of the predominating NNE-SSW-trending faulting in Claritas Fossae have been determined by Smith et al. (2009) to range between 3.3 and 2.5 Ga using the fault-buffered crater counting method. This age was later confirmed by Vaz et al. (2014).

At the regional scale, the topography of Claritas Fossae is dominated by the N020W-trending steep scarp of Claritas Rupes (Fig. 1b). This scarp, locally exceeding 2000 m in height (Fig. 1c), has been likely formed during the last stage of the main phase of the Thaumasia tectonics in the Late Hesperian or Early Amazonian (Tanaka and Davis, 1988; Balbi et al., 2024) and was interpreted as the surface expression of a crustal-scale listric normal fault that led to the formation of the present regional half-graben morphology (Hauber and Kronberg, 2005; Balbi and Marini, 2024; Balbi et al., 2024). The Claritas Rupes scarp divides the Claritas Fossae region into a western, ~ 300 km-long and ~ 80 km-wide depression and the eastern Claritas Fossae highlands (Fig. 1b). The large-scale depression extends between 21°S and 25°S and it is superimposed on the floor of a large extensional structure, informally termed Thaumasia Graben by Hauber and Kronberg (2005). The floor of the depression is inclined by $\sim 1^\circ$ towards the east. The Thaumasia Graben floor is generally characterized by a smooth surface with a low amount

of textural details when compared to the surrounding areas.

South of 24°S , Hauber and Kronberg (2005) described three WNW-ESE-trending topographic highs resembling ridges and consisting of rugged Noachian crust (Fig. 1b). One of these ridges constitutes the topographical boundary of the studied Thaumasia Graben depression to the south and separates the western lowlands of Claritas Fossae into two segments (Fig. 1b). In the southern segment, small-scale volcanoes of LCP-rich composition have been previously identified (Pieterik et al., 2024). Their structural relationship with the NNE-SSW-trending faults evidences that volcanic activity postdates the faulting. This suggests that the formation of this volcanic field occurred in the period spanning through the Late Hesperian and the Early Amazonian. However, as some of these volcanoes show fresh morphological appearance, this suggests that they might be younger, from the Middle/Late Amazonian period (Pieterik et al., 2024). In addition to local volcanism, there is evidence that Thaumasia also experienced regional-scale volcanism (Dohm and Tanaka, 1999; Grott et al., 2007) (Fig. 1b). One of the large-scale volcanoes located in Coracis Fossae indicates that they are older than 3.9 Ga (Grott et al., 2005), as they are cut by rift-related faults.

Previously it was also proposed that some parts of Thaumasia (namely area from 39°S to 42°S) might experience processes associated with glaciation as glacial landforms have been described within large impact craters (e.g., Rossi et al., 2011). Moreover, the formation of the Syria-Thaumasia block was considered as a potential result of a regional detachment along a volcanically-buried layer of ice (Cassanelli and Head, 2019). However, the required rapid accumulation of volcanic material for the proposed surficial glaciovolcanic origin was unlikely and therefore this scenario is not favored.

3. Data and methods

To search for and map the fresh-appearing scarps and associated features, we performed a visual inspection and analysis of data based on two satellite image datasets: Context Camera (CTX, 5–6 m/pixel; Malin et al., 2007) and HiRISE (25–50 cm/pixel; McEwen et al., 2007), both on board NASA's Mars Reconnaissance Orbiter (MRO) spacecraft. For the initial identification of regions of interest, we used a global CTX mosaic of Mars rendered at 5 m/pixel of spatial resolution and released by the Bruce Murray Laboratory for Planetary Visualization (Dickson et al., 2023). These observations were supplemented by observations of individual HiRISE images downloaded from the Planetary Data System (PDS) Geoscience Node (Table S1). A combination of these two datasets is well-suited to conduct such local-scale geological investigation, including the identification and characterization of small-scale features which were the main target of this study. In the framework of this research, we only focused on those features that either have a sharp scarp trace and thin ridges formed by the scarp shoulders and/or display clear structural relationships with present-day surficial processes and their deposits (Fig. S1). Besides observations of linear features, we defined the boundaries of constructional and flow-like units by tracking grey-scale and textural variations within the CTX images. In addition to these image datasets, we used Thermal Emission Imaging System (THEMIS; Edwards et al., 2011) data to describe the regional context of the study area and identify regional-scale features that provide insights for our interpretations. To provide regional topographical profiles and maps, we used global elevation data acquired from a blended Digital Elevation Model (DEM) with spatial resolution of 200 m/pixel (Ferguson et al., 2018) derived from the Mars Orbiter Laser Altimeter (MOLA; Smith et al., 2001) and the High Resolution Stereo Camera (HRSC; Gwinner et al., 2016) on board Mars Express spacecraft. Due to the small size of investigated features, the spatial resolution of MOLA-HRSC DEM is insufficient to conduct a detailed topographic analysis. Therefore, to define structural relationships between identified features (scarps) and units (lava flows) for the selected regions of interest within the studied area we used DEMs derived from CTX stereo pair images (DEM with ground sampling distance of ~ 12 m and vertical accuracy of ~ 4 m; for

details see Table S2). The production of CTX-based DEMs has been achieved by applying a data processing information system called MarsSI (Mars System of Information) specifically designed to manage and process Martian satellite data on demand (Quantin-Nataf et al., 2018). All image and data analysis associated with visualization, mapping, and stratigraphic relationships were conducted using ArcGIS software via ArcMap and ArcScene versions 10.5. Due to the fact that on Mars very few studies described similar-looking features so far, we used terrestrial analogs of fresh scarps developed on mountain slopes accompanied by present-day slope processes to provide a comparative morphological analysis. Terrestrial counterparts were looked for in the literature and the selected examples were identified in images obtained from Google Earth™ (Google Inc, 2021) based on Maxar satellite imagery.

4. Observations and results

4.1. Characteristics of linear features

At the Claritas Rupes scarp and on the Thaumasia Graben floor, we identified fresh-appearing, small-scale scarps that are morphologically distinct relative to the surrounding tectonic features, and are spatially associated with depression centers. Along the base of Claritas Rupes, we distinguished two depression centers, a northern and a southern one with dimensions of approximately 38×105 km and 28×85 km, respectively (Fig. 2a). The two depressions are bounded to the east by

the base of the Claritas Rupes scarp and are separated from each other by a large elevated block (Fig. 2a). The southern depression center on the western side is bounded by a topographic scarp (Fig. 2a), whereas the northern depression center is bounded to the west by a gently uprising slope. The eastern boundary of the northern depression continues towards the southwestern direction into the central part of the Thaumasia Graben and is highlighted by pristine-looking scarps (Fig. 2b). These northwest-facing scarps separate low plains in the west and northwest and an elevated structural block in the east (Fig. 2c-d). The scarps are associated with constructional mounds partially dissected by these scarps (Fig. 2e), and are characterized by well-defined traces and sharp and thin ridges formed by the scarp shoulders.

The majority of pristine scarps on the main slope of Claritas Rupes are located above and to the east of the depression centers (Fig. 2a). In particular, based on the CTX-based DEM, we found that the western shoulders of the scarps rise above the inferred average slope of the main scarp (Fig. 3a). Thus, the identified scarps are uphill-facing (antislope) and display pristine morphologies, without evidence of significant modification by erosion or being covered by aeolian deposits. They are characterized by fine details of the scarp trace, and the sharp and thin ridges formed by the scarp shoulders (Fig. 3b-f). Using HiRISE images, we found that boulders that have been broken off from the top of the main scarp of Claritas Rupes were often stopped by the uphill-facing scarps causing their accumulation (Fig. 3). In some places, where these uphill-facing scarps are not present or less well developed, the boulders were capable of moving further downslope, forming flow lobes

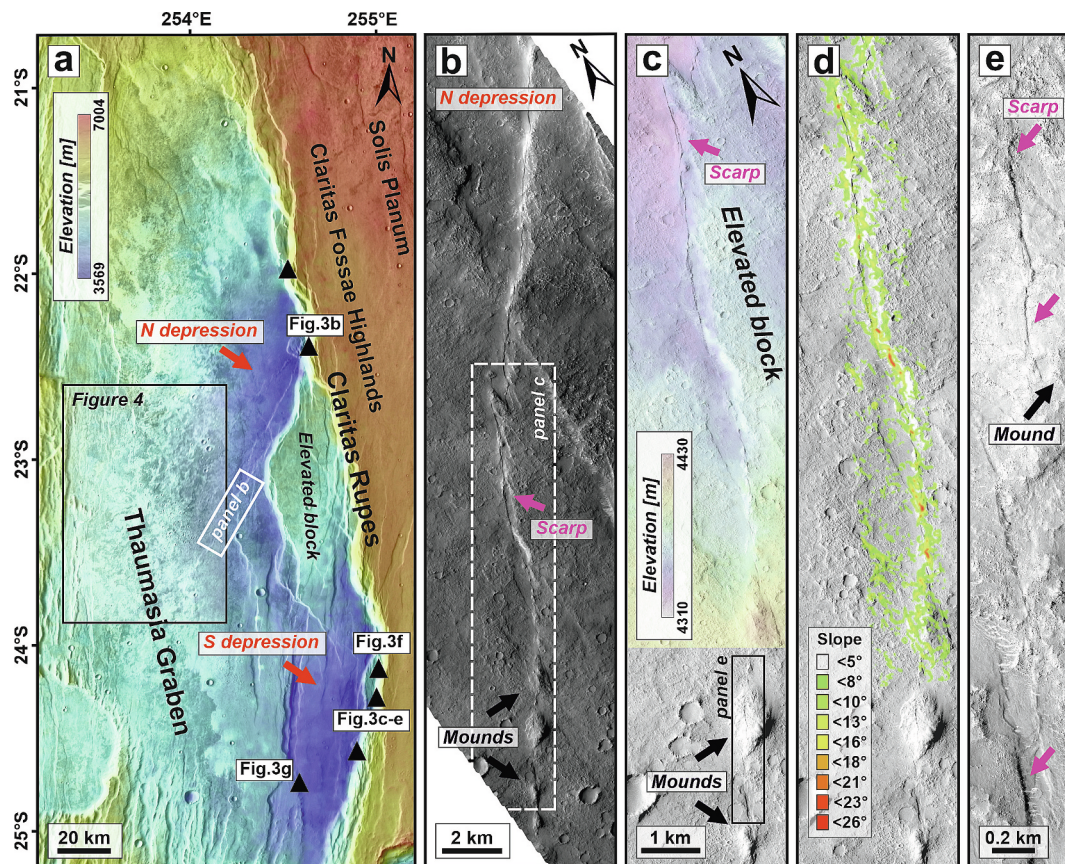


Fig. 2. (a) A sketch topographic map of the studied region including the western Thaumasia Graben and eastern Claritas Fossae highlands with locations of the detailed figures (zoom-in of Fig. 1b). The black triangles indicate the locations of investigated fresh-looking scarps mostly located at the Claritas Rupes scarp (see Fig. 3). (b) The CTX image of the central part of the Thaumasia Graben shows fresh-appearing NE-SW-trending scarps associated with <1 km size mounds. (c) Zoom-in CTX image of the studied scarps, partially overlaid by the corresponding CTX-based DEM showing that the southeastern side of the fault is topographically elevated in relation to the northeastern side of the scarp. Produced using stereo-pair of CTX images G22_026933_1569 and N13_067509_1587, centered at $\sim 22^\circ$ S, $\sim 254^\circ$ E. (d) The corresponding slope map of the studied scarp. (e) Zoom-in of HiRISE image (ESP_080130_1565, centered at 23.471° S, 254.133° E) showing cross-cutting relationships between the mapped faults and mounds aligned to the fault strike.

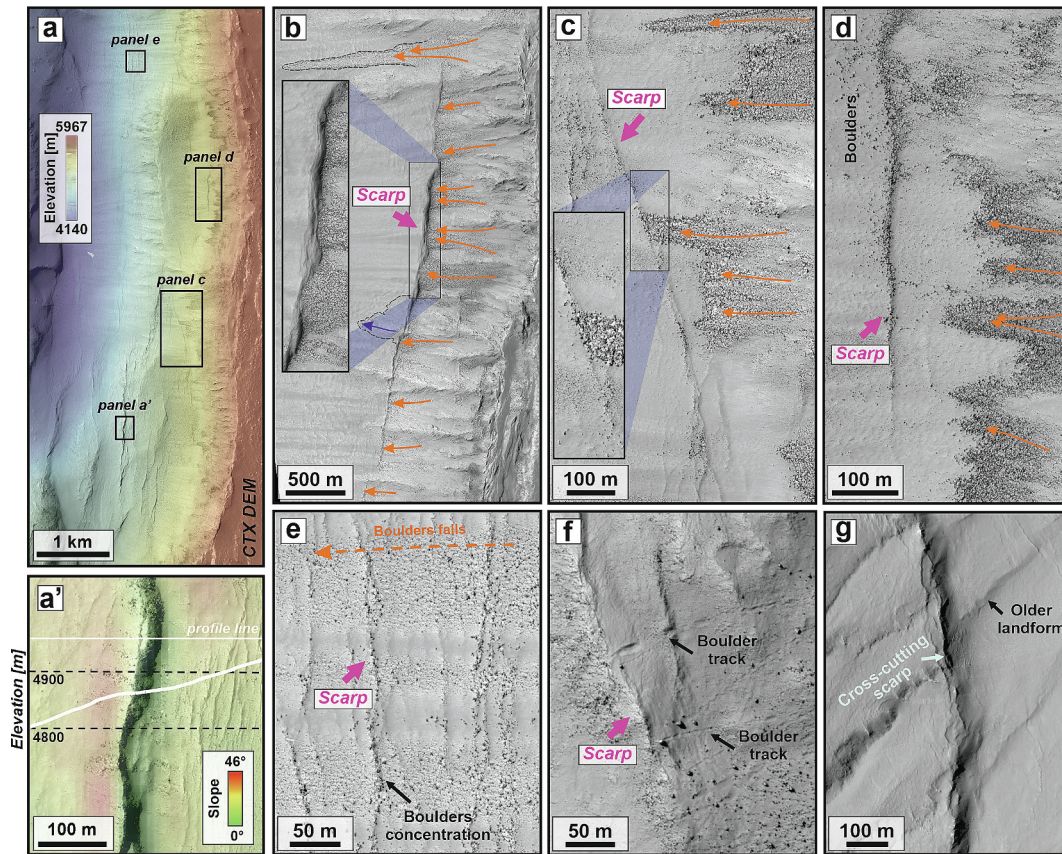


Fig. 3. (a) A topographic image of the Claritas Rupes scarp affected by the elongated uphill-facing scarps and downslope moving boulders. Produced using CTX stereo-pair images P18_007945_1532 and N10_066414_1533, centered at $\sim 25.8^{\circ}\text{S}$, $\sim 255.2^{\circ}\text{E}$. (a') The corresponding zoom-in image of fresh-looking fault overlaid by the slope map and corresponding topographic profile showing textural smothering at the fault surface. Produced using the same CTX-based DEM. See Fig. 2a for location. (b–e) Examples of fresh-looking scarps mapped within the studied region at the Claritas Rupes scarp. Details of uphill-facing scarps that stopped and accumulated boulders along their strike. Orange solid lines with arrows indicate the downslope direction of boulder movement. (e) Cluster of scarps developed on the main scarp of Claritas Rupes that has been partially covered by a concentrated stream of boulders (or rock debris). The scarp trends are highlighted by the accumulation of boulders. (f) Close-up image of the boulders and their tracks that have been stopped at the antislope scarp. (g) An example of a pristine scarp situated parallel to the predominant in the studied region N-S trending scarps. In addition, this scarp crosscuts the associated NE-SW features of most likely lithified aeolian-origin landforms. In the particular region, the scarp bounds the western side of the southern depression center (see Fig. 2a for location). The HiRISE images: (b) ESP_078218_1575, centered at 22.484°S , 254.689°E ; (c–e) PSP_007945_1555, centered at 24.334°S , 255.008°E ; (f) ESP_078508_1555, centered at 24.072°S , 255.032°E ; (g) ESP_081686_1550, centered at 24.946°S , 254.596°E . All images are north-oriented and the image details are provided in Table S1.

with high concentrations of boulders (Fig. 3b–d). However, even in such cases, a higher concentration of boulders highlights the antislope of these scarps. In addition to the uphill-facing scarps located on the main Claritas Rupes scarp, we found a fresh-looking scarp on the opposite, western side of the southern depression center (Fig. 3g). This feature is parallel to the dominating N-S trending fault scarps and crosscuts the associated, likely lithified, aeolian-origin deposits (Fig. 3g).

4.2. Topographic landforms on the Thaumasia Graben floor

In addition to linear features, we also found landforms with irregular plan view shapes that form constructional, flow-like units at the floor of the Thaumasia Graben. The elongations of these flow-like units follow the general topographic trend of the east-inclined graben (Fig. 4a). Topographic profiles reveal thicknesses of these units ranging from ~ 30 to 40 m (Fig. 4b). Moreover, some of them are linked to small-scale hollows (~ 2.5 km in length) that are spatially associated with a channel from which flow units originate (Fig. 4c). We also observed channels that are dispersed throughout the studied region as well as well-preserved flow-like units, whose boundaries are sometimes difficult to map as most of the units have overlapping relationships (Fig. 4d–f). Additionally, we identified a conical-shaped constructional landform associated with a central depression and flow-like structures in the

central part of the studied region (Fig. 5). Based on the relatively high number of impact craters on these surfaces, the flow-like units are much older than the identified linear features.

5. Discussion

5.1. Neotectonics at Claritas Rupes scarp

Our observations revealed the presence of uphill-facing scarps on the Claritas Rupes scarp. On Earth, the formation of such scarps is often attributed to Deep-seated Gravitational Slope Deformations (DGSDs; Soldati, 2013) or instabilities related to glacial retreat (Crosta et al., 2013) (Fig. 6a–c). For Mars, glacial retreat has been suggested to explain the morphology of some ridges showing crestal grabens and antislope scarps in the Valles Marineris (e.g., Melas–Candor chasma boundary; Fig. 6d–e) (Mège and Bourgeois, 2011; Makowska et al., 2016; Discenza et al., 2021). The Thaumasia region has likely experienced glacial processes in the past as well (Rossi et al., 2011; Cassanelli and Head, 2019), however, the study area does not show any signs of past glaciation(s) as no glacial landforms have been observed (i.e., Pieterek et al., 2024). Therefore, neither glacial-induced DGSDs nor post-glacial uplift (Jarman, 2006) can readily explain the presence of uphill-facing scarps in this geological setting, although we cannot fully exclude them.

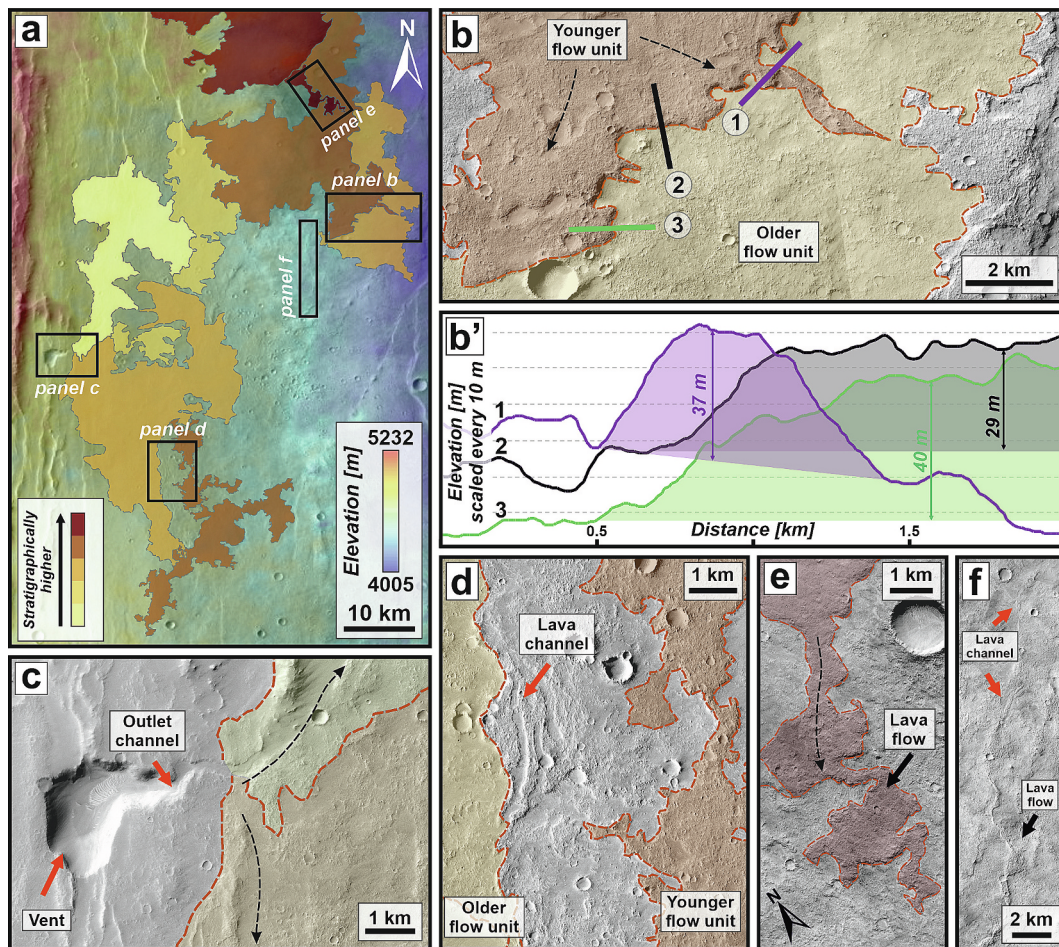


Fig. 4. (a) Sketch map of the central part of the study area with potential volcanic units on the floor of the Thaumasia Graben. Unit colours represent stratigraphic position, with lower units being lighter and overlying units being darker. The base map is a blend of a DEM derived from the MOLA-HRSC and a global CTX mosaic. (b) The easternmost part of the Thaumasia Graben floor shows the overlapping thick lava flows with irregular outlines. A CTX-based DEM (CTX stereo-pair G22_026933_1569 and N13_067509, centered at $\sim 22^{\circ}\text{S}$, $\sim 254^{\circ}\text{E}$) was used to produce profiles across the outer margin of the flow shown in panel (b'). The dashed lines mark the presumed propagation direction of the lava flows. (c) Volcanic vent with east- and northeast-trending outlet channel associated with flow units spreading out from the channel (CTX image D16_033302_1571, centered at 23.01°S , 253.26°E). (d) Overlapping flow units emplaced south to the vent, characterized by irregular outlines with channel (CTX image F04_037271_1566, centered at 23.50°S , 253.70°E). (f) An example of small-scale volcanic features such as a lava channel and associated flow units that are common throughout the studied region (CTX image G23_027355_1558, centered at 24.26°S , 254.15°E).

The formation of uphill-facing scarps can also be attributed to toppling when layers are steeply inclined (Hippolyte et al., 2006; Yokoyama, 2020). However, this formation mechanism can be excluded, as in the upper sections of the main scarp of Claritas Rupes sub-horizontal layers are exposed. Besides these processes, uphill-facing scarps could represent antithetic normal faults formed simultaneously or after the formation of the main crustal-scale fault of Claritas Rupes in the Late Hesperian/Early Amazonian (Tanaka and Davis, 1988). However, such scenario seems unlikely due to the pristine morphology of the identified scarps (Fig. 6f-h). If these scarps had an age of 3 Ga, they should be completely covered by deposits released from surrounding steep walls or significantly eroded. Although erosion rates on Mars are very low in the Amazonian, given the thin atmosphere and absence of liquid water (e.g., Golombek et al., 2006; Vaz et al., 2014), a period of three billion years would provide enough time to alter the appearance of these morphologically subtle surface features significantly. Finally, the formation of these scarps could be also related to slope gravitational processes (e.g., rotational sliding; Varnes, 1978), but our search for similar features on other steep-sided slopes in Tharsis (i.e., inside slope of volcanic calderas of Tharsis Montes or Olympus Mons) do not show any evidence of the formation of morphologically similar scarps on the caldera walls. Hence, this scenario seems to be also unlikely.

Nevertheless, the DGSDs characterized by uphill-facing scarps are also often recognized on Earth in seismically active mountain regions (Soldati, 2013 and references therein). In such geological settings, their development is generally related to tensional stresses induced by gravity at steep-sided slopes and triggered by the presence of discontinuities of tectonic origin and/or seismic activity (Moro et al., 2007; Gutiérrez et al., 2008). These factors seem favorable in the context of the tectonic evolution of the study region and therefore represent a plausible scenario for the development of the observed scarps.

However, whatever the exact cause of small-scale faulting on the Claritas Rupes scarp is, we suggest that tectonic movements are responsible for the formation of these pristine uphill-facing scarps in the study region. Altogether, the pristine topography (sharp and thin ridges), spatial distribution (association with depression centers), and geological context of the tectonically active Claritas Fossae region, the studied uphill-facing scarps lead us to interpret them as surficial expressions of tectonic activity. We asserted that the ongoing subsidence of the two depression centers developed as halfgraben (northern) and full graben (southern) would have occurred through normal dip slip faulting along the main Claritas Rupes fault. Such a process caused the Claritas Rupes scarp to become locally even topographically higher, and therefore more unstable. This may result in the DGSDs causing the formation

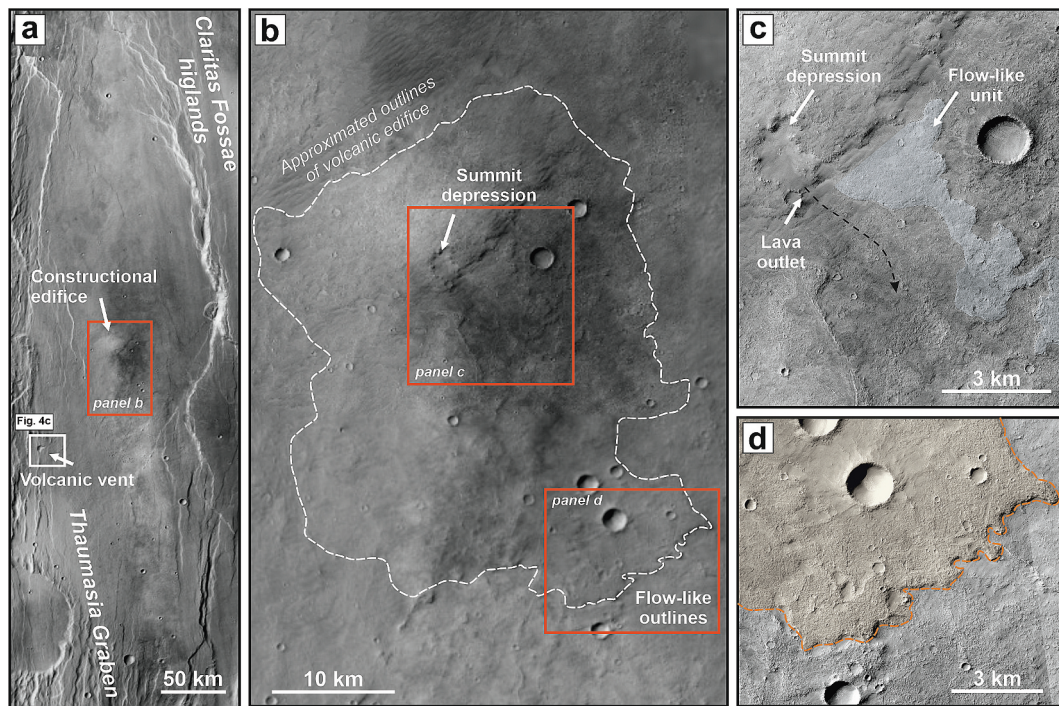


Fig. 5. (a) CTX mosaic (centered at 24.26°S and 254.15°E) covering part of the Thaumasia Graben and the northern depression, characterized by a smooth surface relative to the adjacent terrains. A constructional edifice with a central summit depression resembling a volcano can be seen in the central part. (b) Zoom-in image of this potential volcano with approximate outlines of the edifice. (c) Close-up image of the summit part of the edifice with a central depression accompanied by a flow-like unit (based on CXT image G23_027355_1558). (d) Example of flow-like outlines of the approximate outer boundary of the volcanic edifice. Based on CXT images G23_027355_1558 and G22_026933_1569 (Table S1). North is up in all panels.

of the uphill-facing scarps identified in this research. We therefore interpret the scarps as morphologic expressions of normal faults.

5.2. Age of scarps

The comparison of the morphological appearance of the discovered faults with previous features detected elsewhere on Mars (Fig. 6i-k) indicates that faulting at Claritas Rupes is likely younger than most of the other recent Martian faulting. The scarps are well-preserved and their morphology is not modified by significant accumulations of dust or boulders released from surrounding steep slopes. However, in the case of Martian small-scale linear structures, determining their absolute ages is difficult or even impossible due to the limitations of the crater counting method (Warner et al., 2015; Palucis et al., 2020; Wang et al., 2020). Therefore, the best approach for constraining the age of the formation is a relative dating method, which uses crosscutting relationships with landforms that are a result of present-day Martian surface processes; such as dunes, landslide deposits, talus cones, or boulder avalanche deposits. For example, Kumar et al. (2019) identified fresh-appearing faults at the Coprates Chasma scarp and studied the crosscutting relationships between the faults and the talus cones and other debris flow material (Fig. 6i), suggesting that the tectonic activity postdates the slope processes. Moreover, similar observations based on HiRISE images have been made by Roberts et al. (2012), who found a ~100 m-length fault offsetting the colluvium on the scarp of the Cerberus Fossae graben. Beneath this fault, the scarp has been affected by boulder tracks that have been not covered by the aeolian deposits indicating that they are relatively recent. Cross-cutting relationships may be also coupled with model age determination through crater counting. Spagnuolo et al. (2011) identified a 1.9 Myr landslide associated with a dune field. Since the landslide is cut by the fault, tectonic activity must be younger than the landslide formation. This structural observation suggests recent tectonic activity accompanied by subsidence inside the Aureum Chaos region.

In this study, we were unable to make an absolute age determination and therefore we used relative dating methods based on present-day surface processes. We found that boulders moving downslope are stopped at, and accumulated along, fresh-looking uphill-facing scarps (Fig. 3). In some cases, the boulder tracks are distinguishable at the HiRISE images as they were not yet erased by the slope processes (Fig. 3e) suggesting a very recent time of their formation (Sinha et al., 2020). Continuous and intense mass wasting processes at the Claritas Rupes scarp, where the rate of downslope moving material must be high due to the steep slopes, should quickly fill the accommodation space created by the uphill-facing scarps (Fig. 7). If the scarps were geologically old (> millions of years), these depressions should be already filled by rockfall deposits and in such case boulders would easily move further downhill due to the gravity (Fig. 3a and e). As the consequence, these small uphill-facing scarps would be covered and precluded from possible identification. A comparable process of sediment accumulation against uphill-facing slopes is known on Earth where it is related to the neotectonic activity (Bowman and Gerson, 1986; Persaud and Pfiffner, 2004). Moreover, the pristine appearance of the faults (Fig. 3), as visible in image observations and topographic profiles (Fig. 3a'), suggests that the tectonic activity responsible for the fault formation is so young that slope movements and aeolian processes have not yet erased their evidence. Our inferences are consistent with the results of De Haas et al. (2013) who implied that typical small-scale morphology on Mars may be subdued within <1 Myr.

These morphological constraints are further supplemented by the fresh appearance of boulders accumulated along the identified scarps. Assuming the Martian global erosional rate ($\sim 10^{-8}$ m/yr) in the Amazonian period (Golombek et al., 2006; Vaz et al., 2014), the average-sized boulders (2–3 m in diameter) should be destroyed in <300 Myr. Such age range of the boulders' lifetime is consistent with estimations for other planetary bodies as well (Schröder et al., 2021; Noma and Hirata, 2024). Even though, the observed boulders reveal an angular shape indicating negligible erosion. Therefore, we estimated the

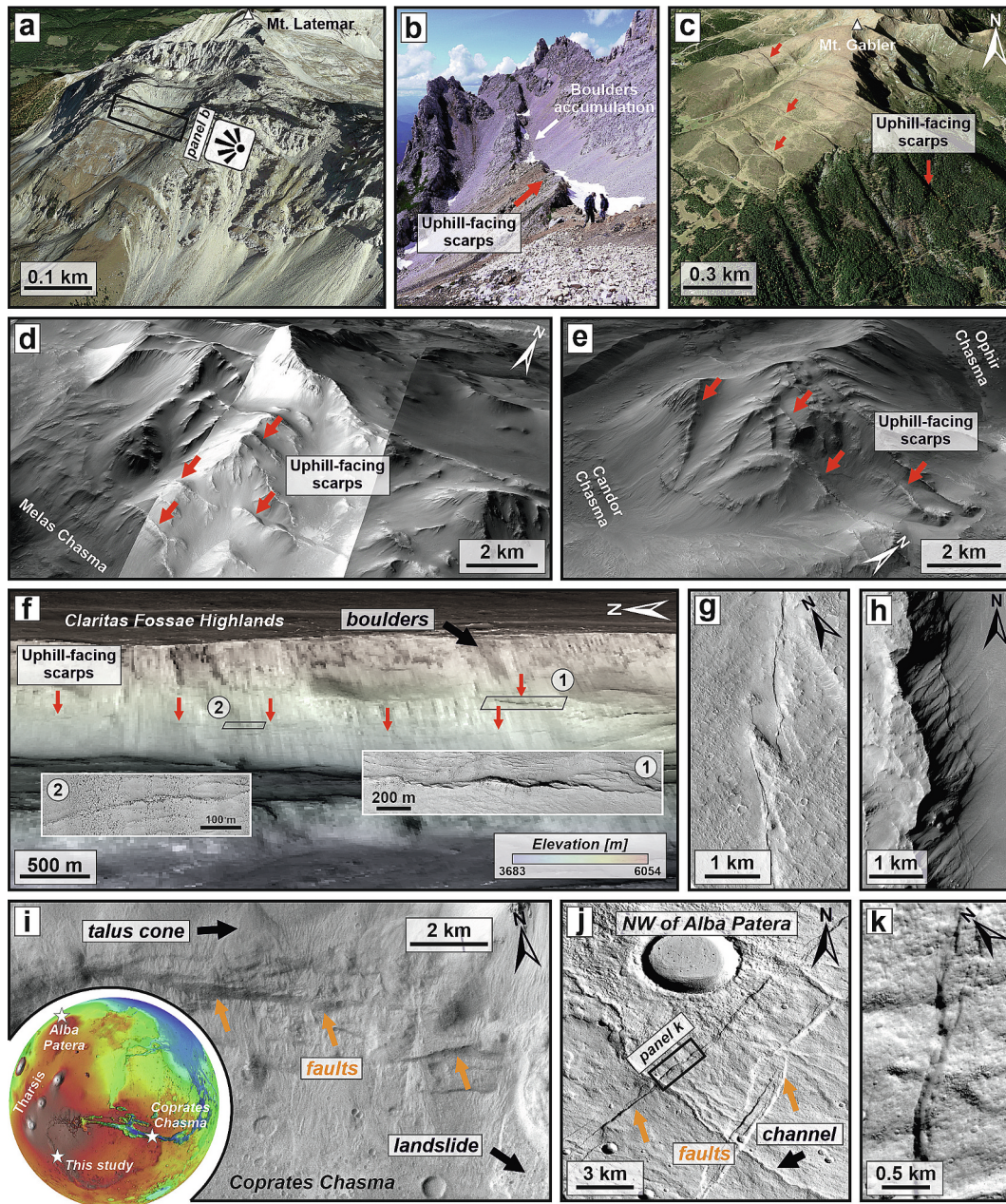


Fig. 6. (a) Google Earth™ visualization of Monte Latemar in northern Italy (Alto Adige/Trentino; $46^{\circ}22'21.4''N$, $11^{\circ}33'12.5''E$) with uphill-facing scarps. (b) Field image from the SW slope of Monte Latemar presenting the scarp that stops and accumulates downslope moving boulders. (c) The Google Earth™ 3D visualization of the Monte Gabler in Italy ($46^{\circ}41'23.6''N$ $11^{\circ}45'46.6''E$) with uphill-facing scarps. For more detailed description, the reader is referred to [Crosta et al. \(2013\)](#). (d-e) Examples of the uphill-facing scarps identified in Valles Marineris at the boundary between Melas-Candor chasma boundary (d) and Candor-Ophir chasma boundary (e). Produced with Google Earth™ Pro software using the MOLA gridded elevation data and CTX images. (f) The 3D visualization of the main fault scarp bounding the Claritas Fossae highlands and Thaumasia Graben (the reader is referred to [Fig. 2a](#)). Produced using the CTX-based DEM (P18_007945_1532 and N10_066414_1533, centered at $\sim 25.8^{\circ}S$, $\sim 255.2^{\circ}E$). The insets show the HiRISE images of selected faults common at the Claritas Rupes fault scarp marked by the red arrows (PSP_007945_1555, centered at $24.33^{\circ}S$, $255.00^{\circ}E$). (g-h) Examples of the pristine faults observed in the studied region (CTX image G03_019430_1553, centered at $24.72^{\circ}S$, $254.57^{\circ}E$). (i) Young faults of the eastern part of Coprates Chasma cross-cutting the talus cones and other debris material ([Kumar et al., 2019](#)). Produced using CTX image F17_042531_1661, centered at $13.79^{\circ}S$, $299.15^{\circ}E$. The inset shows the topographic map of Mars with the white stars indicating the locations of the studies documenting pristine faults on Mars. (j) Morphologically pristine faults in the NW region of Alba Mons described by [Karimova et al. \(2017\)](#). Produced using CTX image P20_008736_2272, centered at $47.33^{\circ}N$, $246.43^{\circ}E$. The zoom-in image of the fault is presented in panel (k). (For interpretation of the references to colour in this figure legend, the reader is referred to the web version of this article.)

formation age of uphill-facing scarps developed at Claritas Rupes to be <1 Myr and implied a very young age of the uphill-facing scarp formation.

In general, a disturbance of regolith or frequent boulder movements are possible signs of former tectonic activity (e.g., [Roberts et al., 2012](#); [Kumar et al., 2019](#); [Watters et al., 2019](#)). Although we can assert that the

studied faults have to be very young, we did not observe any boulder bounce-associated ejecta-like patterns such as those observed by [Vijayan and Harish \(2022\)](#) across Mars. Such features are created during boulder falls and have a very short preservation time. Based on global observations in various geotectonic settings, it was proposed that the presence of bounce-associated ejecta-like patterns indicates that the rockfall had

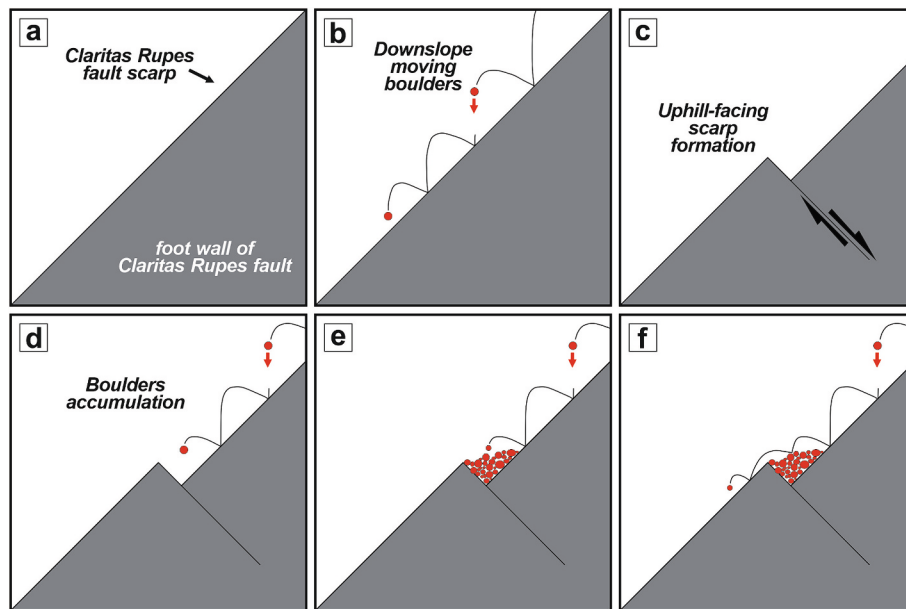


Fig. 7. Schematic drawing presenting the formation of uphill-facing scarps at Claritas Rupes fault scarp in relation to downslope moving boulders before (a-b) and after their development (d-f). Not to scale.

occurred not more than ~ 2 to 4 Mars years (~ 4 –8 Earth years) before the respective image had been taken (Vijayan and Harish, 2022). The lack of boulder bounce ejecta identified in this study may indicate that this region has not experienced any major blockfall activity since at least the year 2004–2000, and therefore, Claritas Rupes may not have experienced any tectonic movements that triggered blockfalls at least since the year 2000.

In addition to rockfalls, detailed mapping revealed that the fault development on the western scarp of the southern depression center (Fig. 2a) postdates the formation of SW-NE-aligned lithified aeolian structures (Figs. 3g and 6h). As the identified scarps show a pristine morphology, we argue that their age is much younger than the main Thaumasia faulting. Thus, the observed stratigraphic relationship implies a relatively young age of the identified fault development most likely associated with the subsidence of the southern depression center. Altogether, these observations indicate that the neotectonic activity responsible for the youngest faults in the Claritas Rupes region had to be very recent.

Although present-day seismicity (Stähler et al., 2022; Ceylan et al., 2023) and perhaps even very recent volcanic activity (Horvath et al., 2021) has been found to be associated with the Cerberus Fossae region within Elysium Planitia, comparable surface evidence of contemporary endogenous processes elsewhere on Mars is rare. To date, no direct surface or morphological evidence of present-day endogenous processes (i.e., newly emplaced volcanic deposits, new fault traces in before-and-after images) has been observed. However, several sites have been proposed to display extremely pristine and well-preserved faults (Fig. 6), supporting the notion of a relatively recent formation (Spagnuolo et al., 2011; Karimova et al., 2017; Kumar et al., 2019). Our findings suggest that endogenous activity in the Claritas Fossae region may not have completely ceased and that this region may be another center of activity where relatively young endogenous activity caused modification of the Martian surface (cf. Knapmeyer et al., 2023).

5.3. Volcanic resurfacing and young faulting on the Thaumasia Graben floor

The floor of the Thaumasia Graben seems to have experienced younger resurfacing event(s) relative to the predominating Thaumasia faulting (dated between 3.4 and 2.5 Ga; Smith et al., 2009; Vaz et al.,

2014), as parts of its surface lack evidence of N-S trending large-scale scarps and grabens that are ubiquitous elsewhere in the Claritas Fossae region (Fig. 2a). We infer that these tectonic structures have been likely buried by the observed flow-like units (Fig. 4) that share morphological similarities with lava flows elsewhere on Mars (e.g., Bleacher et al., 2007; Hauber et al., 2011; Peters et al., 2021; Wiedeking et al., 2023). In addition, the mapped flows are associated with a small-scale depression and a channel propagating downslope, as well as with a constructional edifice (Fig. 5) which resembles Martian shield volcanoes (Hauber et al., 2009). The thickness of the mapped units is similar to that of lava flows documented elsewhere in Tharsis (e.g., Peters et al., 2021). Based on these observations, we conclude that the ancient, highly fractured terrains might have been covered by younger volcanic products associated with Hesperian/Amazonian volcanism that infilled the floor of the Thaumasia Graben (Fig. 4), which is in contact with the base of the Claritas Rupes scarp. Although we could only identify one certain (Fig. 4c) and one plausible (Fig. 5) volcanic source in the western and central part of the Thaumasia Graben depressions, we cannot fully discard the presence of additional volcanic vents that have been buried under younger lava flows.

These observations imply the loading of the old heavily fractured crust by younger volcanic products within the Thaumasia Graben. On Earth, volcanic loading or magma chamber discharge may cause significant subsidence at the Earth's surface over an extended period after the eruption (Leng and Zhong, 2010; Browning and Gudmundsson, 2015; Huppert et al., 2015), which is accommodated at the surface by faulting. It should be noted, however, that the volcanic landforms on the floor of the Thaumasia Graben are relatively densely cratered, and hence are likely older than the identified uphill-facing scarps, making a direct geological link unlikely. Although the volcanic activity in Thaumasia Graben likely did not trigger the formation of the studied faults, we cannot fully discard this scenario. It might be plausible that volcanic loading or magma chamber discharge might have been causing time-extended subsidence of the Thaumasia Graben floor until the Late Amazonian epoch (Fig. 1c).

In addition to kilometer-sized lava flows (Fig. 4), we also documented small-scale, < 1 km-sized mounds that form circular to elongated constructional edifices resembling volcanic landforms. The mounds are associated with fresh-looking scarps in the central part of the Thaumasia Graben (Fig. 2b-e). They are aligned along the fault strike (NE-SW),

partially showing crosscutting relationships, and therefore, their formation might have been associated with the fault development. The NE-SW-trending fault scarps likely constitute the continuation of the southeastern boundary of the northern depression center (Fig. 2a-b). The topographical offset along this scarp caused the southeastern shoulder to form an elevated block (Fig. 2c). As for the fault-related surfaces, however, the observed features are too small to determine the absolute model ages of their formation. Our morphological observations indicate that the fault has been formed after or simultaneously with the volcanic mound formation, as often observed on Earth, for example in the Shixi area in China (Yiming et al., 2022) or in the Oka-taina volcanic center in New Zealand (Berryman et al., 2022). Therefore, in the geological context of this study and the entire Claritas Fossae region, these observations suggest that the tectonic events responsible for the formation of these faults may be genetically linked to small-scale volcanic events operating within this region. However, their relationship to the uphill-facing fault scarps located on the main Claritas Rupes scarp remains unknown.

The NE-SW alignment of both the faults and associated mounds might constitute the prolongation of a set of topographic scarps extending from the northern depression center and a landslide emplaced

at the base of the Claritas Rupes scarp (Fig. 2a-b). Considering the pristine appearance and the relationships of both fault systems, located on the Claritas Rupes main scarp and within the Thaumasia Graben, two temporal scenarios of their formation can be considered. Assuming the co-activity of both fault systems at the same/similar time, it can be asserted that tectonic activity was associated with and probably triggered by local volcanic activity. However, we interpret this scenario as less plausible as no evidence for cross-cutting relationships for the NE-SW-trending scarps with recent surface landforms was observed. Additionally, the direction of their alignment suggests a structural link with the large elevated block that divides two depression centers in Thaumasia Graben. Therefore, we consider it more likely that two independent tectonic events occurred, with the uphill-facing fault scarps on the main Claritas Rupes scarp being the youngest set of faults within the studied region, caused by neotectonic movements.

5.4. Young fault formation in the context of Claritas Fossae tectonics

The region of Claritas Fossae is a long-lived volcano-tectonic region on Mars whose endogenic activity is thought to have started in the Early to Middle Noachian. The activity declined during the Late Noachian and

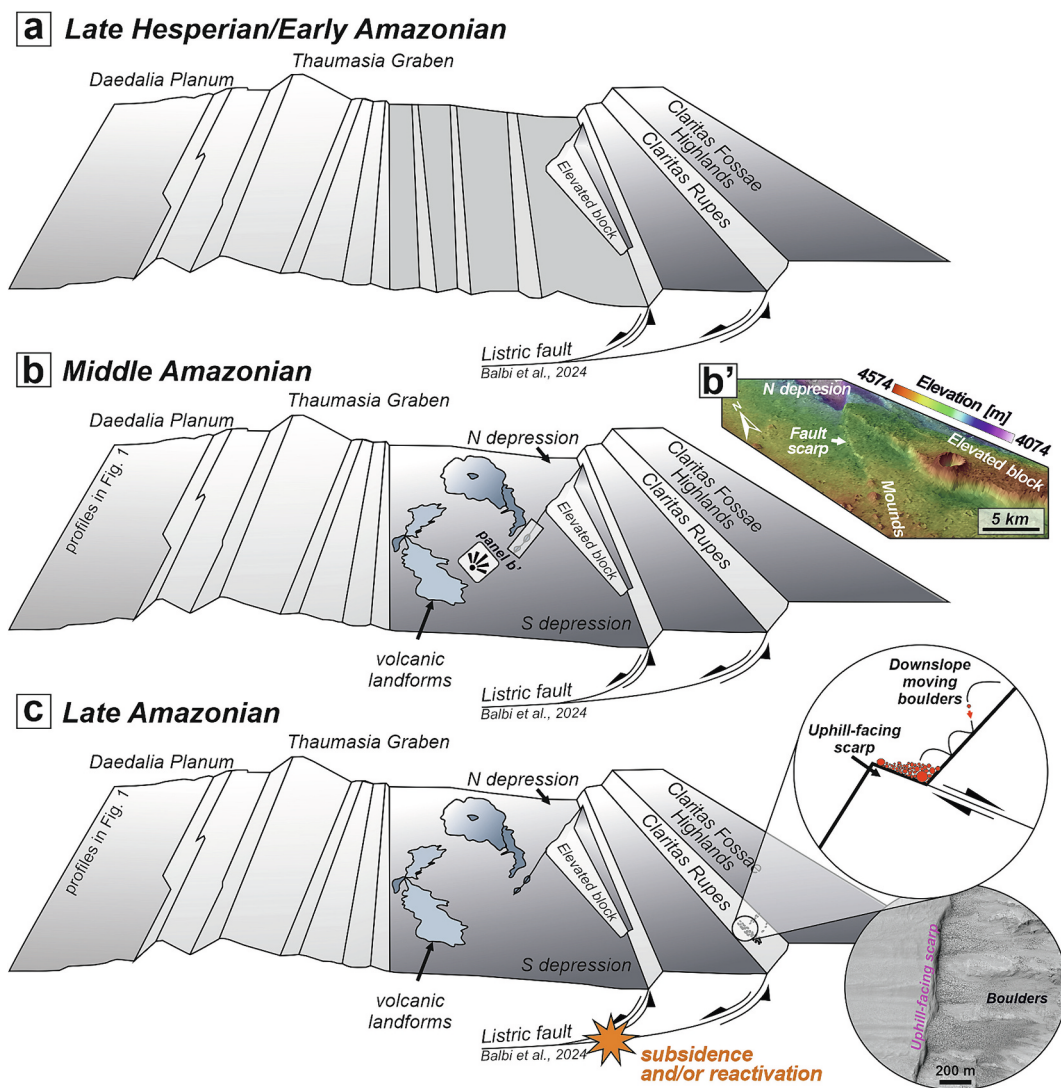


Fig. 8. Schematic representation of the geological context of the study area in the Late Hesperian/Early Amazonian (a) with visualizations of two-event scenario that led to the development of the identified fresh-appearing scarp associated with plausible volcanic-origin mounds inside the Thaumasia Graben in Middle Amazonian (b) and the formation of pristine uphill-facing scarps with boulders accumulation along their strike at the Claritas Rupes main scarp in the Late Amazonian (c). The reader is referred to the text for a more detailed discussion about the evolution of the Claritas Rupes scarp and Thaumasia Graben.

Early Hesperian, and progressively decreased further during the Late Hesperian/Amazonian (Tanaka and Davis, 1988; Dohm and Tanaka, 1999; Anderson et al., 2001; Balbi et al., 2024). In the regional context, past (ancient) endogenic processes are expressed on the surface both as tectonic (Grott et al., 2005, 2007; Hauber and Kronberg, 2005; Smith et al., 2009; Vaz et al., 2014; Balbi et al., 2024) and volcanic (Dohm and Tanaka, 1999; Pieterrek et al., 2024) landforms. Until now, no evidence of neotectonics has been reported for the Thaumasia region. Our observations of very young fault scarps (<1 Myr) indicate that some internal dynamics in the Claritas Fossae region remained active until the Late Amazonian (Fig. 8). Specifically, faulting at the Claritas Rupes scarp may have continued to the Late Amazonian and might have been associated with the tectonic activity (subsidence) responsible for the formation of depression centers on the Thaumasia Graben floor.

Volcanic resurfacing of the floor of the Thaumasia Graben and associated loading might have possibly triggered some crustal subsidence and localized faulting. However, as demonstrated in this study, this may not have been the trigger for the very recent faulting at the Claritas Rupes scarp, as the volcanic landforms are less pristine and relatively densely cratered, hence older than the uphill-facing fault scarps. In this study, we show that volcanic deposits have covered the Thaumasia Graben floor, burying the main N-S trending grabens of the Claritas Fossae region (Fig. 8b) before the formation of the newly identified small-scale faults within the graben.

The small size of the identified landforms prevents providing precise temporal constraints. The uncertain structural relationship and likely age difference between the features on the floor of Thaumasia Graben and those at the Claritas Rupes scarp makes it difficult to relate their formation to a common cause. Therefore, we suggest that at least two tectonic events are responsible for their formation. An earlier event led to the emplacement of local volcanic deposits on the floor of Thaumasia Graben. These deposits are associated with coeval or younger faulting. At least one of these younger faults has a NE-SW orientation (Fig. 8b). It is parallel to a regional set of structural lineaments which were interpreted by Balbi and Marini (2024) and Balbi et al. (2024) as Riedel shears associated with dextral transtensional displacement along a NNW-SSE-trending shear corridor roughly parallel to the Claritas Rupes scarp. Dextral shear at the Claritas Rupes scarp has also been proposed by Webb and Head III (2002) and Montgomery et al. (2009) to accommodate gravity-driven movement of the Thaumasia block to the south and east. A second, younger faulting event is associated with the formation of the uphill-facing scarps at the Claritas Rupes main scarp (Fig. 3). The scarps are spatially associated with depression centers on the Thaumasia Graben floor at the base of Claritas Rupes (Figs. 2 and 8c).

Based on relative dating, we inferred that the NE-SW-trending faults on the floor of Thaumasia Graben (Figs. 2b-e and 8b) postdates the Late Hesperian/Early Amazonian volcano-tectonic activity and could be related to tectonic movements at Riedel shears, associated with small-volume volcanic activity. On the other hand, the pristine scarps associated with boulder accumulations at Claritas Rupes scarp (Fig. 3) have been developed very recently, most likely <1 Ma. Such faulting might be caused by DGSDs released by seismic activity related to ongoing subsidence of the depression centers at the base of the Claritas Rupes scarp and/or a reactivation of the listric Claritas Rupes fault (Fig. 8c), which has been formed in the Late Hesperian/Early Amazonian (Balbi et al., 2024).

Such interpretation implies that although endogenic processes in Claritas Fossae have been most intense in the Noachian and Hesperian (Dohm and Tanaka, 1999; Anderson et al., 2001; Balbi et al., 2024), the Thaumasia Graben and its eastern border fault, the Claritas Rupes scarp may have remained active, even though at low rates, producing very young structures (Fig. 8). This conclusion appears to be consistent with global thermal modelling revealing a current zone of relatively high degrees of partial melting in the mantle beneath the Claritas Fossae/Rupes region (Plesa et al., 2023) that might coexist or even induce the

interpreted neotectonic activity in the Claritas Fossae region. Nevertheless, the still uncertain stratigraphic relationship between the identified scarps indicates a persistent need for conducting dedicated research for small-scale scarps within this region that would address the recent unknowns. A more detailed structural mapping, temporal constraints, and search for deglaciation evidence would be critical in better constraining the Amazonian-age evolution of Claritas Fossae.

6. Conclusions

We present evidence for very young endogenic activity in the southeastern part of Tharsis. The activity is manifest in the form of very young faults (<1 Ma), sub-km-sized scarps at the Claritas Rupes scarp. Our morphological mapping revealed a local system of pristine-appearing, uphill-facing fault scarps, which are spatially associated with depression centers partially filled by volcanic deposits. As shown by the spatial relationships between the faults and present-day surficial processes such as rockfalls, the tectonic activity is so young that slope and aeolian processes have not yet erased their evidence. We link the formation of these faults with DGSDs related to ongoing subsidence of depression centers at the base of the Claritas Rupes scarp and/or reactivation of the listric normal fault that is morphologically expressed as the Claritas Rupes scarp. Altogether, the study region has been affected by long-lasting volcano-tectonic activity, with the possibility that this area might be still tectonically active even today.

CRedit authorship contribution statement

Bartosz Pieterrek: Writing – review & editing, Writing – original draft, Visualization, Software, Project administration, Methodology, Investigation, Data curation, Conceptualization. **Petr Brož:** Writing – review & editing, Validation, Supervision, Conceptualization. **Ernst Hauber:** Writing – review & editing, Validation, Supervision, Conceptualization.

Declaration of competing interest

The authors declare that they have no known competing financial interests or personal relationships that could have appeared to influence the work reported in this paper.

Data availability statement

The Mars Reconnaissance Orbiter Context Camera (CTX) images used for geological mapping in this study are freely available at the NASA Planetary Data System website (<https://ode.rsl.wustl.edu/mars/>). The global THEMIS-IR day time mosaic image is from Edwards et al. (2011) and the Mars Orbiter Laser Altimeter (MOLA) topographic data blended with the High Resolution Stereo Camera (HRSC) digital elevation model (DEM) used in this work are available in Ferguson et al. (2018). The CTX-based DEM used for topographic measurements and 3D visualizations has been produced using MarsSI (Mars System of Information) – a system designed to process Martian orbital data (Quantin-Nataf et al., 2018). This system is available on the website (<https://marssi.univ-lyon1.fr>). The produced DEM is available at the MARSSI repository or on request from the authors. The shapefiles containing the outlines of geological units that were used to prepare the figures and maps are available in the Supplementary Material to this article.

Acknowledgments

This research was financially supported by the Ministry of Education and Science funding for 2024 in the scheme of publication grant no. 62.9012.2401.00.0 to BP. BP is financially supported by the START 2024 scholarship funded by the Foundation for Polish Science. Elevation

data has been processed using the MarsSI (marssi.univ-lyon1.fr) application funded by the European Union's Seventh Framework Program (FP7/2007-2013) (ERC Grant Agreement No. 280168).

Appendix A. Supplementary data

Supplementary data to this article can be found online at <https://doi.org/10.1016/j.icarus.2024.116198>.

References

- Anderson, R.C., Dohm, J.M., Golombek, M.P., Haldemann, A.F.C., Franklin, B.J., Tanaka, K.L., Lias, J., Peer, B., 2001. Primary centers and secondary concentrations of tectonic activity through time in the western hemisphere of Mars. *J. Geophys. Res. Planets* 106, 20563–20585. <https://doi.org/10.1029/2000JE001278>.
- Andrews-Hanna, J.C., Zuber, M.T., Hauck, S.A., 2008. Strike-slip faults on Mars: observations and implications for global tectonics and geodynamics. *J. Geophys. Res.* 113, E08002. <https://doi.org/10.1029/2007JE002980>.
- Balbi, E., Marini, F., 2024. Lineament domain analysis to unravel tectonic settings on planetary surfaces: insights from the Claritas fossae (Mars). *Geosciences* 14, 79. <https://doi.org/10.3390/geosciences14030079>.
- Balbi, E., Ferretti, G., Tosi, S., Crispini, L., Cianfarra, P., 2024. Polyphase tectonics on Mars: insight from the Claritas fossae. *Icarus* 115972. <https://doi.org/10.1016/j.icarus.2024.115972>.
- Berryman, K., Villamor, P., Nairn, I., Begg, J., Alloway, B.V., Rowland, J., Lee, J., Capote, R., 2022. Volcano-tectonic interactions at the southern margin of the Okataina volcanic centre, Taupo volcanic zone, New Zealand. *J. Volcanol. Geotherm. Res.* 427, 107552. <https://doi.org/10.1016/j.jvolgeores.2022.107552>.
- Bleacher, J.E., Greeley, R., Williams, D.A., Cave, S.R., Neukum, G., 2007. Trends in effusive style at the Tharsis Montes, Mars, and implications for the development of the Tharsis province. *J. Geophys. Res. Planets* 112, 1–15. <https://doi.org/10.1029/2006JE002873>.
- Bouley, S., Baratoux, D., Paulien, N., Misenard, Y., Saint-Bézar, B., 2018. The revised tectonic history of Tharsis. *Earth Planet. Sci. Lett.* 488, 126–133. <https://doi.org/10.1016/j.epsl.2018.02.019>.
- Bowman, D., Gerson, R., 1986. Morphology of the latest quaternary surface-faulting in the Gulf of Elat region, eastern Sinai. *Tectonophysics* 128, 97–119. [https://doi.org/10.1016/0040-1951\(86\)90310-0](https://doi.org/10.1016/0040-1951(86)90310-0).
- Browning, J., Gudmundsson, A., 2015. Surface displacements resulting from magma-chamber roof subsidence, with application to the 2014–2015 Bardarbunga-Holuhraun volcanotectonic episode in Iceland. *J. Volcanol. Geotherm. Res.* 308, 82–98. <https://doi.org/10.1016/j.jvolgeores.2015.10.015>.
- Cailleau, B., Walter, T.R., Janle, P., Hauber, E., 2003. Modeling volcanic deformation in a regional stress field: implications for the formation of graben structures on Alba Patera. *Mars. J. Geophys. Res. Planets* 108, 1–18. <https://doi.org/10.1029/2003je002135>.
- Carr, M.H., Head III, J.W., 2010. Geologic history of Mars. *Earth Planet. Sci. Lett.* 294, 185–203. <https://doi.org/10.1016/j.epsl.2009.06.042>.
- Cassanelli, J.P., Head, J.W., 2019. Glaciovolcanism in the Tharsis volcanic province of Mars: implications for regional geology and hydrology. *Planet. Space Sci.* 169, 45–69. <https://doi.org/10.1016/j.pss.2019.02.006>.
- Ceylan, Savas, Giardini, Domenico, Clinton, J., Kim, Doyeon, Khan, Amir, Stähler, Simon C., Zenhäusern, Géraldine, Lognonné, Philippe, Banerdt, William Bruce, Zürich, E., Zürich, E., Ceylan, S., Giardini, D., Clinton, J.F., Kim, D., Khan, A., Stähler, S.C., Zenhäusern, G., Lognonné, P., Banerdt, W.B., 2023. Mapping the seismicity of Mars with InSight. *J. Geophys. Res. Planets* 128 (8). <https://doi.org/10.1029/2023JE007826> e2023JE007826.
- Crosta, G.B., Frattini, P., Agliardi, F., 2013. Deep seated gravitational slope deformations in the European Alps. *Tectonophysics* 605, 13–33. <https://doi.org/10.1016/j.tecto.2013.04.028>.
- De Haas, T., Hauber, E., Kleinmans, M.G., 2013. Local late Amazonian boulder breakdown and denudation rate on Mars. *Geophys. Res. Lett.* 40, 3527–3531. <https://doi.org/10.1002/grl.50726>.
- Dickson, J.L., Ehlmann, B.L., Kerber, L.H., Fassett, C.I., 2023. Release of the global CTX mosaic of Mars: an experiment in information-preserving image data processing. In: *54th Lunar Planetary Science Conference*, p. 2806.
- Disenza, M.E., Esposito, C., Komatsu, G., Miccadei, E., 2021. Large-scale and deep-seated gravitational slope deformations on Mars: a review. *Geosci.* 11, 1–19. <https://doi.org/10.3390/geosciences11040174>.
- Dohm, J.M., Tanaka, K.L., 1999. Geology of the Thaumasia region, Mars: plateau development, valley origins, and magmatic evolution. *Planet. Space Sci.* 47, 411–431. [https://doi.org/10.1016/s0032-0633\(98\)00141-x](https://doi.org/10.1016/s0032-0633(98)00141-x).
- Dohm, J.M., Tanaka, K.L., Hare, T.M., 2001. Geologic, paleotectonic, and paleoerosional maps of the Thaumasia region, Mars, scale 1:5,000,000. *U.S. Geol. Surv. Geol. Invest. Ser. I-2650*, 3 sheets. URL: <https://pubs.usgs.gov/imap/i2650/>.
- Edwards, C.S., Nowicki, K.J., Christensen, P.R., Hill, J., Gorelick, N., Murray, K., 2011. Mosaicking of global planetary image datasets: 1. Techniques and data processing for Thermal Emission Imaging System (THEMIS) multi-spectral data. *J. Geophys. Res.* E Planets 116, E10008. <https://doi.org/10.1029/2010JE003755>.
- Ferguson, R.L., Hare, T.M., Laura, J., 2018. HRSC and MOLA Blended Digital Elevation Model at 200m v2. [WWW Document]. *Astrogeology PDS Annex*. U.S. Geol. Surv. 6. URL: http://bit.ly/HRSC_MOLA_Blend_v0.
- Giardini, D., Lognonné, P., Banerdt, W.B., Pike, W.T., Christensen, U., Ceylan, S., Clinton, J.F., van Driel, M., Stähler, S.C., Böse, M., Garcia, R.F., Khan, A., Panning, M., Perrin, C., Banfield, D., Beucler, E., Charalambous, C., Euchner, F., Horleston, A., Jacob, A., Kawamura, T., Kedar, S., Mainsant, G., Scholz, J.R., Smrekar, S.E., Spiga, A., Agard, C., Antonangeli, D., Barkaoui, S., Barrett, E., Combes, P., Conejero, V., Daubar, I., Drilleau, M., Ferrier, C., Gabisi, T., Gudkova, T., Hurst, K., Karakostas, F., King, S., Knapmeyer, M., Knapmeyer-Endrun, B., Llorca-Cejudo, R., Lucas, A., Luno, L., Margerin, L., McClean, J.B., Mimoun, D., Murdoch, N., Nimmo, F., Nonon, M., Pardo, C., Rivoldini, A., Manfredi, J.A.R., Samuel, H., Schimmel, M., Stott, A.E., Stutzmann, E., Teanby, N., Warren, T., Weber, R.C., Wiczorek, M., Yana, C., 2020. The seismicity of Mars. *Nat. Geosci.* 13, 205–212. <https://doi.org/10.1038/s41561-020-0539-8>.
- Golombek, M.P., Phillips, R.J., 2010. 5. Mars tectonics. In: *Watters, T.R., Schultz, R.A. (Eds.), Planetary Tectonics*. Cambridge University Press Cambridge, pp. 183–232.
- Golombek, M.P., Grant, J.A., Crumpler, L.S., Greeley, R., Arvidson, R.E., Bell, J.F., Weitz, C.M., Sullivan, R.J., Christensen, P.R., Soderblom, L.A., Squyres, S.W., 2006. Erosion rates at the Mars Exploration Rover landing sites and long-term climate change on Mars. *J. Geophys. Res. Planets* 111, 1–14. <https://doi.org/10.1029/2006JE002754>.
- Grott, M., Hauber, E., Werner, S.C., Kronberg, P., Neukum, G., 2005. High heat flux on ancient Mars: evidence from rift flank uplift at Coracis fossae. *Geophys. Res. Lett.* 32, 1–4. <https://doi.org/10.1029/2005GL023894>.
- Grott, M., Hauber, E., Werner, S.C., Kronberg, P., Neukum, G., 2007. Mechanical modeling of thrust faults in the Thaumasia region, Mars, and implications for the Noachian heat flux. *Icarus* 186, 517–526. <https://doi.org/10.1016/j.icarus.2006.10.001>.
- Gutiérrez, F., Ortuño, M., Lucha, P., Guerrero, J., Acosta, E., Coratza, P., Piacentini, D., Soldati, M., 2008. Late quaternary episodic displacement on a sacking scarp in the central Spanish Pyrenees. Secondary paleoseismic evidence? *Geodin. Acta* 21, 187–202. <https://doi.org/10.3166/ga.21.187-202>.
- Gwinner, K., Jaumann, R., Hauber, E., Hoffmann, H., Heipke, C., Oberst, J., Neukum, G., Ansan, V., Bostelmann, J., Dumke, A., Elgner, S., Erkeling, G., Fueten, F., Hiesinger, H., Hoekzema, N.M., Kersten, E., Loizeau, D., Matz, K.D., McGuire, P.C., Mertens, V., Michael, G., Pasewaldt, A., Pinet, P., Preusker, F., Reiss, D., Roatsch, T., Schmidt, R., Scholten, F., Spiegel, M., Stesky, R., Tirsch, D., Van Gasselt, S., Walter, S., Wählisch, M., Willner, K., 2016. The high resolution stereo camera (HRSC) of Mars express and its approach to science analysis and mapping for Mars and its satellites. *Planet. Space Sci.* 126, 93–138. <https://doi.org/10.1016/j.pss.2016.02.014>.
- Hauber, E., Kronberg, P., 2005. The large Thaumasia graben on Mars: is it a rift? *J. Geophys. Res. Planets* 110, 1–13. <https://doi.org/10.1029/2005JE002407>.
- Hauber, E., Bleacher, J., Gwinner, K., Williams, D., Greeley, R., 2009. The topography and morphology of low shields and associated landforms of plains volcanism in the Tharsis region of Mars. *J. Volcanol. Geotherm. Res.* 185, 69–95. <https://doi.org/10.1016/j.jvolgeores.2009.04.015>.
- Hauber, E., Broz, P., Jagert, F., Jodowski, P., Platz, T., 2011. Very recent and wide-spread basaltic volcanism on Mars. *Geophys. Res. Lett.* 38, 1–5. <https://doi.org/10.1029/2011GL047310>.
- Hippolyte, J.C., Brocard, G., Tardy, M., Nicoud, G., Bourlès, D., Braucher, R., Ménard, G., Souffaché, B., 2006. The recent fault scarps of the Western Alps (France): tectonic surface ruptures or gravitational sacking scarps? A combined mapping, geomorphic, levelling, and ¹⁰Be dating approach. *Tectonophysics* 418, 255–276. <https://doi.org/10.1016/j.tecto.2006.02.009>.
- Horleston, A.C., Clinton, J.F., Ceylan, S., Giardini, D., Charalambous, C., Irving, J.C.E., Lognonné, P., Stähler, S.C., Zenhäusern, G., Dahmen, N.L., Duran, C., Kawamura, T., Khan, A., Kim, D., Plasman, M., Euchner, F., Beghein, C., Beucler, E., Huang, Q., Knapmeyer, M., Knapmeyer-Endrun, B., Lekić, V., Li, J., Perrin, C., Schimmel, M., Schmeer, N.C., Stott, A.E., Stutzmann, E., Teanby, N.A., Xu, Z., Panning, M., Banerdt, W.B., 2022. The far side of Mars: two distant Marsquakes detected by InSight. *Seism. Rec.* 2, 88–99. <https://doi.org/10.1785/0320220007>.
- Horvath, D.G., Moitra, P., Hamilton, C.W., Craddock, R.A., Andrews-Hanna, J.C., 2021. Evidence for geologically recent explosive volcanism in Elysium. *Icarus* 365, 114499. <https://doi.org/10.1016/j.icarus.2021.114499>.
- Huppert, K.L., Royden, L.H., Perron, J.T., 2015. Dominant influence of volcanic loading on vertical motions of the Hawaiian islands. *Earth Planet. Sci. Lett.* 418, 149–171. <https://doi.org/10.1016/j.epsl.2015.02.027>.
- Inc, Google, 2021. Google Earth Pro (Version 7.3.4.8642, software) [WWW Document]. <http://www.google.com/earth>.
- Jarman, D., 2006. Large rock slope failures in the highlands of Scotland: characterisation, causes and spatial distribution. *Eng. Geol.* 83, 161–182. <https://doi.org/10.1016/j.enggeo.2005.06.030>.
- Karimova, R., Hauber, E., Crown, D., Platz, T., Berman, D., Scheidt, S., Weitz, C., 2017. Fault populations on Alba Mons, Mars, and their age relationships to volcanic, fluvial, and glacial processes. In: *European Planetary Science Congress*. EPSC2017-207-1.
- Knapmeyer, M., Stähler, S., Plesa, A.C., Ceylan, S., Charalambous, C., Clinton, J., Dahmen, N., Duran, C., Horleston, A., Kawamura, T., Kim, D., Li, J., Plasman, M., Zenhäusern, G., Weber, R.C., Giardini, D., Panning, M.P., Lognonné, P., Banerdt, W. B., 2023. The global seismic moment rate of Mars after event S1222a. *Geophys. Res. Lett.* 50, 1–9. <https://doi.org/10.1029/2022GL102296>.
- Krishnan, V., Kumar, P.S., 2022. Long-lived and continual volcanic eruptions, tectonic activity, pit chains formation, and Boulder avalanches in northern Tharsis region: implications for late Amazonian geodynamics and Seismo-tectonic processes on Mars. *J. Geophys. Res. Planets* 128. <https://doi.org/10.1029/2022JE007511> e2022JE007511.

- Kumar, S.P., Krishna, N., Prasanna Lakshmi, K.J., Raghukanth, S.T.G., Dhabu, A., Platz, T., 2019. Recent seismicity in Valles Marineris, Mars: insights from young faults, landslides, boulder falls and possible mud volcanoes. *Earth Planet. Sci. Lett.* 505, 51–64. <https://doi.org/10.1016/j.epsl.2018.10.008>.
- Leng, W., Zhong, S., 2010. Surface subsidence caused by mantle plumes and volcanic loading in large igneous provinces. *Earth Planet. Sci. Lett.* 291, 207–214. <https://doi.org/10.1016/j.epsl.2010.01.015>.
- Lognonné, P., Banerdt, W.B., Clinton, J., Garcia, R.F., Giardini, D., Knapmeyer-Endrun, B., Panning, M., Pike, W.T., 2023. Mars seismology. *Annu. Rev. Earth Planet. Sci.* 51, 643–670. <https://doi.org/10.1146/annurev-earth-031621-073318>.
- Makowska, M., Mège, D., Gueydan, F., Chéry, J., 2016. Mechanical conditions and modes of paraglacial deep-seated gravitational spreading in Valles Marineris, Mars. *Geomorphology* 268, 246–252. <https://doi.org/10.1016/j.geomorph.2016.06.011>.
- Malin, M.C., Bell, J.F., Cantor, B.A., Caplinger, M.A., Calvin, W.M., Clancy, R.T., Edgett, K.S., Edwards, L., Haberle, R.M., James, P.B., Lee, S.W., Ravine, M.A., Thomas, P.C., Wolff, M.J., 2007. Context camera investigation on board the mars reconnaissance orbiter. *J. Geophys. Res. Planets* 112. <https://doi.org/10.1029/2006JE002808>. E05S04.
- McEwen, A.S., Eliason, E.M., Bergstrom, J.W., Bridges, N.T., Hansen, C.J., Delamere, W. A., Grant, J.A., Gulick, V.C., Herkenhoff, K.E., Keszthelyi, L., Kirk, R.L., Mellon, M.T., Squyres, S.W., Thomas, N., Weitz, C.M., 2007. Mars reconnaissance Orbiter's high resolution imaging science experiment (HiRISE). *J. Geophys. Res.* 112, E05S02. <https://doi.org/10.1029/2005JE002605>.
- Mège, D., Bourgeois, O., 2011. Equatorial glaciations on Mars revealed by gravitational collapse of Valles Marineris wall-slopes. *Earth Planet. Sci. Lett.* 310, 182–191. <https://doi.org/10.1016/j.epsl.2011.08.030>.
- Montgomery, D.R., Som, S.M., Jackson, M.P.A., Schreiber, B.C., Gillespie, A.R., Adams, J. B., 2009. Continental-scale salt tectonics on Mars and the origin of Valles Marineris and associated outflow channels. *Bull. Geol. Soc. Am.* 121, 117–133. <https://doi.org/10.1130/B26307.1>.
- Moro, M., Saroli, M., Salvi, S., Stramondo, S., Doumaz, F., 2007. The relationship between seismic deformation and deep-seated gravitational movements during the 1997 Umbria-Marche (Central Italy) earthquakes. *Geomorphology* 89, 297–307. <https://doi.org/10.1016/j.geomorph.2006.12.013>.
- Mouginis-Mark, P.J., Crown, D.A., Zimbelman, J.R., Williams, D.A., 2021. 3 - The Tharsis Province. In: Crown, D.A., Mouginis-Mark, P.J., Gregg, T.K.P. (Eds.), Zimbelman, J. R. Elsevier, *The Volcanoes of Mars*, pp. 36–68. <https://doi.org/10.1016/B978-0-12-822876-0.00013-8>.
- Noma, M., Hirata, N., 2024. Investigation of boulder distribution in (1) Ceres and insight into its surface evolution. *Icarus* 414, 116031. <https://doi.org/10.1016/j.icarus.2024.116031>.
- Palucis, M.C., Jasper, J., Garczynski, B., Dietrich, W.E., 2020. Quantitative assessment of uncertainties in modeled crater retention ages on Mars. *Icarus* 341, 113623. <https://doi.org/10.1016/j.icarus.2020.113623>.
- Persaud, M., Pfiffner, O.A., 2004. Active deformation in the eastern Swiss Alps: post-glacial faults, seismicity and surface uplift. *Tectonophysics* 385, 59–84. <https://doi.org/10.1016/j.tecto.2004.04.020>.
- Peters, S.I., Christensen, P.R., Clarke, A.B., 2021. Lava flow eruption conditions in the Tharsis Volcanic Province on Mars. *J. Geophys. Res. Planets* 126. <https://doi.org/10.1029/2020JE006791>.
- Pieterrek, B., Ciazela, J., Lagain, A., Ciazela, M., 2022. Late Amazonian dike-fed distributed volcanism in the Tharsis volcanic province on Mars. *Icarus* 386, 115151. <https://doi.org/10.1016/j.icarus.2022.115151>.
- Pieterrek, B., Brož, P., Hauber, E., Stephan, K., 2024. Insight from the Noachian-aged fractured crust to the volcanic evolution of Mars: A case study from the Thaumasia graben and Claritas Fossae, 407, 115770. <https://doi.org/10.1016/j.icarus.2023.115770>.
- Plesa, A.C., Padovan, S., Tosi, N., Breuer, D., Grott, M., Wieczorek, M.A., Spohn, T., Smrekar, S.E., Banerdt, W.B., 2018. The thermal state and interior structure of Mars. *Geophys. Res. Lett.* 45, 12,198–12,209. <https://doi.org/10.1029/2018GL080728>.
- Plesa, A.C., Wieczorek, M., Knapmeyer, M., Rivoldini, A., Bozdog, E., Walterova, M., Knapmeyer-Endrun, B., Kim, D., Broquet, A., Stähler, S., Mittelholz, A., Breuer, D., Johnson, C.L., Hauber, E., Panning, M., Spohn, T., Lognonné, P., Smrekar, S.E., Banerdt, W.B., 2023. InSight Science Team, 2023. InSight's constraints on the interior of Mars: Geodynamical models and observations. In: 54th Lunar Planetary Science Conference, p. 2212.
- Quantin-Nataf, C., Lozac, L., Thollot, P., Loizeau, D., Bultel, B., Fernando, J., Allemand, P., Dubuffet, F., Poulet, F., Ody, A., Clenet, H., Leyrat, C., Harrison, S., 2018. MarsSI: Martian surface data processing information system. *Planet. Space Sci.* 150, 157–170. <https://doi.org/10.1016/j.pss.2017.09.014>.
- Richardson, J.A., Bleacher, J.E., Connor, C.B., Glaze, L.S., 2021. Small volcanic vents of the Tharsis Volcanic Province, Mars. *J. Geophys. Res. Planets* 126. <https://doi.org/10.1029/2020JE006620> e2020JE006620.
- Rivas-Dorado, S., Ruiz, J., Romeo, I., 2022. Giant dikes and dike-induced seismicity in a weak crust underneath Cerberus Fossae, Mars. *Earth Planet. Sci. Lett.* 594, 117692. <https://doi.org/10.1016/j.epsl.2022.117692>.
- Roberts, G.P., Matthews, B., Bristow, C., Guerrieri, L., Vetterlein, J., 2012. Possible evidence of paleomarsquakes from fallen boulder populations, Cerberus Fossae. *Mars. J. Geophys. Res. Planets* 117, 1–17. <https://doi.org/10.1029/2011JE003816>.
- Rossi, A.P., van Gasselt, S., Pondrelli, M., Dohm, J., Hauber, E., Dumke, A., Zegers, T., Neukum, G., 2011. Evolution of periglacial landforms in the ancient mountain range of the Thaumasia highlands. *Mars. Geol. Soc. Spec. Publ.* 356, 69–85. <https://doi.org/10.1144/SP356.5>.
- Schröder, S.E., Carsenty, U., Hauber, E., Schulzeck, F., Raymond, C.A., Russell, C.T., 2021. The Boulder population of asteroid 4 Vesta: size-frequency distribution and survival time. *Earth Sp. Sci.* 8. <https://doi.org/10.1029/2019EA000941> e2019EA000941.
- Schultz, R.A., Tanaka, K.L., 1994. Lithospheric-scale buckling and thrust structures on Mars: the Coprates rise and south Tharsis ridge belt. *J. Geophys. Res.* 99, 8371–8385. <https://doi.org/10.1029/94JE00277>.
- Sinha, R.K., Rani, A., Conway, S.J., Vijayan, S., Basu Sarbadhikari, A., Massé, M., Mangold, N., Bhardwaj, A., 2020. Boulder fall activity in the Jezero crater, Mars. *Geophys. Res. Lett.* 47, 1–10. <https://doi.org/10.1029/2020GL090362>.
- Smith, D.E., Zuber, M.T., Frey, H.V., Garvin, J.B., Head, J.W., Muhleman, D.O., Pettengill, G.H., Phillips, R.J., Solomon, S.C., Zwally, H.J., Banerdt, W.B., Duxbury, T.C., Golombek, M.P., Lemoine, F.G., Neumann, G.A., Rowlands, D.D., Aharonson, O., Ford, P.G., Ivanov, A.B., Johnson, C.L., McGovern, P.J., Abshire, J.B., Afzal, R.S., Sun, X., 2001. Mars orbiter laser altimeter: experiment summary after the first year of global mapping of Mars. *J. Geophys. Res. Planets* 106, 23,689–23,722. <https://doi.org/10.1029/2000JE001364>.
- Smith, M.R., Gillespie, A.R., Montgomery, D.R., Batbaatar, J., 2009. Crater-fault interactions: a metric for dating fault zones on planetary surfaces. *Earth Planet. Sci. Lett.* 284, 151–156. <https://doi.org/10.1016/j.epsl.2009.04.025>.
- Soldati, M., 2013. In: Bobrowsky, P.T. (Ed.), *Deep-Seated Gravitational Slope Deformation BT - Encyclopedia of Natural Hazards*. Springer, Netherlands, Dordrecht, pp. 151–155. https://doi.org/10.1007/978-1-4020-4399-4_86.
- Spagnuolo, M.G., Rossi, A.P., Hauber, E., van Gasselt, S., 2011. Recent tectonics and subsidence on Mars: hints from Aureum Chaos. *Earth Planet. Sci. Lett.* 312, 13–21. <https://doi.org/10.1016/j.epsl.2011.09.052>.
- Stähler, S.C., Khan, A., Bruce Banerdt, W., Lognonné, P., Giardini, D., Ceylan, S., Drilleau, M., Al, E., 2021. Seismic detection of the martian core. *Science* (80-) 373, 443–448. <https://doi.org/10.1126/science.abi7730>.
- Stähler, S.C., Mittelholz, A., Perrin, C., Kawamura, T., Kim, D., Knapmeyer, M., Zenhäusern, G., Clinton, J., Giardini, D., Lognonné, P., Banerdt, W.B., 2022. Tectonics of Cerberus Fossae unveiled by marsquakes. *Nat. Astron.* 6, 1376–1386. <https://doi.org/10.1038/s41550-022-01803-y>.
- Stähler, S.C., Dahmen, N., Zenhäusern, G., Ceylan, S., Clinton, J., Duran, C., Horleston, A., Kawamura, T., Kim, D., Giardini, D., Lognonné, P., Mittelholz, A., 2024. One model to rule them all: making sense of Marsquake types and distances. In: 55th Lunar and Planetary Science Conference, p. 2641.
- Tanaka, K.L., Davis, P.A., 1988. Tectonic history of the Syria Planum province of Mars. *J. Geophys. Res.* 93. <https://doi.org/10.1029/jb093i12p14893>.
- Varnes, D.J., 1978. Slope movement types and processes. *Spec. Rep.* 176, 11–33.
- Vaz, D.A., Spagnuolo, M.G., Silvestro, S., 2014. Morphometric and geometric characterization of normal faults on Mars. *Earth Planet. Sci. Lett.* 401, 83–94. <https://doi.org/10.1016/j.epsl.2014.05.022>.
- Vijayan, S., Harish Kimi, K.B., Tuhi, S., Vigneshwaran, K., Sinha, R.K., Conway, S.J., Sivaraman, B., Bhardwaj, A., 2022. Boulder fall ejecta: present day activity on Mars. *Geophys. Res. Lett.* 49, 1–9. <https://doi.org/10.1029/2021GL096808>.
- Wang, Y., Xie, M., Xiao, Z., Cui, J., 2020. The minimum confidence limit for diameters in crater counts. *Icarus* 341, 113645. <https://doi.org/10.1016/j.icarus.2020.113645>.
- Warner, N.H., Gupta, S., Calef, F., Grindrod, P., Boll, N., Goddard, K., 2015. Minimum effective area for high resolution crater counting of martian terrains. *Icarus* 245, 198–240. <https://doi.org/10.1016/j.icarus.2014.09.024>.
- Watters, T.R., Weber, R.C., Collins, G.C., Howley, I.J., Scherrer, N.C., Johnson, C.L., 2019. Shallow seismic activity and young thrust faults on the moon. *Nat. Geosci.* 12, 411–417. <https://doi.org/10.1038/s41561-019-0362-2>.
- Webb, B.M., Head III, J.W., 2002. Noachian tectonics of Syria Planum and the Thaumasia plateau. In: *Lunar and Planetary Science Conference*, p. 1358.
- Wiedeking, S., Lentz, A., Pasckert, J.H., Raack, J., Schmedemann, N., Hiesinger, H., 2023. Rheological properties and ages of lava flows on Alba Mons, Mars. *Icarus* 389, 115267. <https://doi.org/10.1016/j.icarus.2022.115267>.
- Yiming, A., Bian, B., Liu, L., Chen, H., Shan, X., Li, A., Yi, J., 2022. Types and eruption patterns of the carboniferous volcanic edifices in the Shixi area, Junggar Basin. *Front. Earth Sci.* 10, 1–11. <https://doi.org/10.3389/feart.2022.906782>.
- Yokoyama, O., 2020. Evolution of uphill-facing scarps by flexural toppling of slate with high-angle faults. *Geomorphology* 352, 106977. <https://doi.org/10.1016/j.geomorph.2019.106977>.
- Zenhäusern, G., Stähler, S.C., Clinton, J.F., Giardini, D., Ceylan, S., Garcia, R.F., 2022. Low-frequency Marsquakes and where to find them: Back azimuth determination using a polarization analysis approach. *Bull. Seismol. Soc. Am.* 112, 1787–1805. <https://doi.org/10.1785/0120220019>.

Update

Icarus

Volume 420, Issue , 15 September 2024, Page

DOI: <https://doi.org/10.1016/j.icarus.2024.116220>



Contents lists available at [ScienceDirect](#)

Icarus

journal homepage: www.elsevier.com/locate/icarus



Corrigendum

Corrigendum to “Recent faulting at the Claritas Rupes scarp on Mars” [Icarus, 420 (2024), 116198].



Bartosz Pieterek^{a,b,*}, Petr Brož^c, Ernst Hauber^d

^a Polish Geological Institute – National Research Institute, Warsaw, Poland

^b Geohazard Lab, Institute of Geology, Adam Mickiewicz University, Poznań, Poland

^c Institute of Geophysics of the Czech Academy of Sciences, Prague, Czech Republic

^d Institute of Planetary Research, DLR, Berlin, Germany

The authors regret making a mistake by reporting the wrong affiliation of the first author (B. Pieterek) on Page 1: “Polish National Institute – National Science Institute, Warsaw, Poland” which should be

changed to “Polish Geological Institute – National Research Institute, Warsaw, Poland”.

The authors would like to apologise for any inconvenience caused.

DOI of original article: <https://doi.org/10.1016/j.icarus.2024.116198>.

* Corresponding author at: Polish Geological Institute – National Research Institute, Poland.

E-mail address: bpieterek94@gmail.com (B. Pieterek).

<https://doi.org/10.1016/j.icarus.2024.116220>

Available online 19 July 2024

0019-1035/© 2024 The Author(s). Published by Elsevier Inc. This is an open access article under the CC BY-NC-ND license (<http://creativecommons.org/licenses/by-nc-nd/4.0/>).